

# MODIFIED FUZZY C-MEANS CLUSTERING FOR AUTOMATIC TONGUE BASE TUMOUR EXTRACTION FROM MRI DATA

Trushali Doshi<sup>1</sup>, John Soraghan<sup>1</sup>, Derek Grose<sup>2</sup>, Kenneth MacKenzie<sup>2</sup>, Lykourgos Petropoulakis<sup>1</sup>

<sup>1</sup> Department of Electronic & Electrical Engineering, University of Strathclyde, Glasgow, UK

<sup>2</sup> Beatson Oncology Unit and Royal Infirmary, NHS Greater Glasgow and Clyde, Glasgow, UK

## ABSTRACT

Magnetic resonance imaging (MRI) is a widely used imaging modality to extract tumour regions to assist in radiotherapy and surgery planning. Extraction of a tongue base tumour from MRI is challenging due to variability in its shape, size, intensities and fuzzy boundaries. This paper presents a new automatic algorithm that is shown to be able to extract tongue base tumour from gadolinium-enhanced T1-weighted (T1+Gd) MRI slices. In this algorithm, knowledge of tumour location is added to the objective function of standard fuzzy c-means (FCM) to extract the tumour region. Experimental results on 9 real MRI slices demonstrate that there is good agreement between manual and automatic extraction results with dice similarity coefficient (DSC) of  $0.77 \pm 0.08$ .

**Index Terms**— automatic tumour extraction, fuzzy c-means, Hessian analysis, MRI, throat detection

## 1. INTRODUCTION

In the United Kingdom (UK), around 1,500 people are diagnosed with oropharyngeal tumours each year [1], from which 40 percent comprise tongue base tumours' [2]. Surgery and/or radiation therapy are the standard treatment options for this type of tumours. Extraction of tumour region from medical imaging modality such magnetic resonance imaging (MRI) slices is necessary to assist in radiotherapy and surgery planning. Manually extracting tumours from sequential MRI slices is a time consuming process, subjective and may suffer from human errors. Thus, computer-aided algorithms for extracting tongue base tumour from MRI play an increasing role in radiotherapy and surgery planning in an effort to improve the clinical work. Fig. 1 shows typical gadolinium-enhanced T1-weighted (T1+Gd) MRI slice with a visible tongue base tumour. Note that due to gadolinium-enhancement tumour region appear bright as compared to normal region and have high intensity values than normal region but less intensity values than fatty region. Automatic extraction of tongue base tumours from MRI is relatively challenging due to variability in its geometry, presence of adjacent region such as throat and MRI artifacts. Thus, proper selections of

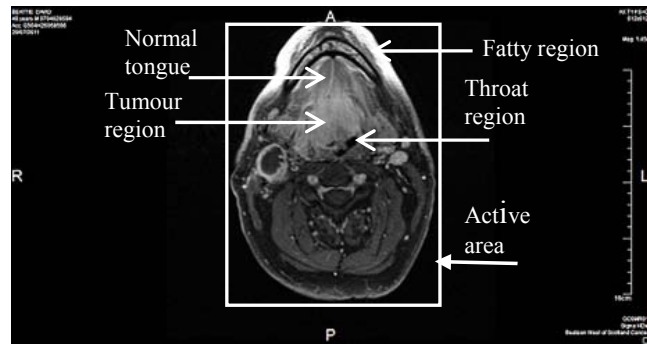


**Fig.1.** Gadolinium-enhanced T1-weighted (T1+Gd) MRI slice with visible tongue base tumour

preprocessing and extraction techniques are vital to obtain satisfactory results.

Existing techniques proposed for the extraction of tongue tumour from medical imaging are either semi-automatic [3] or requires different weighted (T1, T2 and proton density) magnetic resonance (MR) images [4]. The algorithm described in [5] for brain tumour segmentation on T1+Gd MR images to assist in radiosurgery planning requires manual interaction to draw the longest diameter of the tumour. These user-interaction steps or requirement of different weighted MR images can be eliminated from the algorithm by modifying parameters or objective function of fuzzy c-means (FCM) clustering. In [6] local neighbourhood information is added in the similarity measure and membership function of FCM technique to reduce its sensitivity to very high noise and to obtain accurate image segmentation. Weighted means are used in the objective function of FCM in [7] to get stable results than standard FCM [8]. However these modified FCM techniques [6, 7] does not integrate knowledge of region of interest (ROI) and thus segment each region in the image. Researchers in [9] compensate for intensity inhomogeneities (IIH) and segment MR image with brain tumour by modifying objective function of FCM clustering. This modified FCM technique only works with MR images corrupted with salt and pepper noise and cannot compensate for severe IIH. MR images used for this work suffer from severe IIH and therefore IIH correction method and modified FCM technique are applied separately to extract the tumour region.

This paper presents a new fully automatic algorithm to

extract visible tongue base tumours from T1+Gd MRI slices. This algorithm uses only one weighted MR image and does not require any user-interaction or registration step as compared to previous algorithms [3-5]. In the proposed algorithm the anatomical structure close to the common site of the tumour is detected and is used to add a spatial context to standard FCM thus illustrating the versatility of standard FCM algorithm.

The remainder of the paper is organized as follows; Section 2 describes the proposed algorithm. Section 3 discusses comparison of automatic and manual extraction results. Section 4 presents conclusions of this work and some future work.

## 2. AUTOMATIC TONGUE BASE TUMOUR EXTRACTION ALGORITHM

The proposed algorithm can be divided into three steps i) pre-processing, ii) detection of throat region and iii) extraction of tumour region using modified fuzzy c-means (FCM) clustering.

### 2.1. Pre-processing

The pre-processing step includes data size reduction and intensity inhomogeneity (IIH) correction. The region of interest (ROI) (Fig. 2(a)) is cropped automatically from MRI slice (Fig. 1) to reduce the complexity and processing time of the algorithm using basic techniques like thresholding and knowledge that tumour is present in upper part of the image. First, the active area (Fig. 1) is separated from the rest of the image (black region, patient information) by applying thresholding and selecting the bounding box of largest height. ROI is saved as 10 to 60 percent of height and width of active area.

MR images used for this study are obtained using 16-channel, 29-element phased array coils. These phased array coils and other sources [10] cause “shading” artifact called bias field in MR images. Fig. 2(b) illustrates an estimated bias field from Fig. 2(a). It can be seen that the bias field is complex and this gives rise to severe IIH in MR image. Due to this IIH, pixels belonging to one tissue type have varying intensities. To classify pixels belonging to one tissue type in one cluster, it is necessary to correct this IIH. The method described in [11] is applied to the ROI to correct IIH. This method assumes a multiplicative bias field. The method first roughly estimates the bias field by fitting a fourth order polynomial to tissue pixels excluding background pixels. The bias field is then refined by modeling it as bicubic spline defined by grid of knots evenly spread out across the image by taking into account the value of the bias field at knot locations. The optimization is done by minimizing the local entropy of the ROI starting with knot (k1) in the area of the highest SNR. Then knot (k2) with the next highest SNR is recognized and the entropy of the area under k1 and k2 is minimized. This is repeated until all knots are optimized. For this method knot spacing is selected such that anatomical structures are not included in between knots and the bias field is properly described. For this work



**Fig. 2.** (a) ROI (Cropped image from Fig. 1) (b) estimated bias field for Fig 2(a) (c) IIH corrected image

knot spacing of 60 pixels is used for rows and columns for all images. Fig. 2(c) illustrates the IIH corrected image from Fig. 2(a).

### 2.2. Detection of throat region

Tongue base tumours are adjacent to the throat region. It is imperative to use this information in FCM detection of tumour regions. Detection of throat region from each MRI slice is demanding as the size and intensities of the throat region varies for each slice and it split into two as the slices move down the neck region. A throat region is the region of low intensities in the middle part of the ROI. So, for this task only the middle part of the ROI is considered. The hole filling operation described in [12] is performed on the middle part of the ROI. Hole filling operation is performed as morphological reconstruction by erosion from the borders. For grayscale images, a hole is an area of dark pixels surrounded by lighter pixels. The purpose of this operation is to make throat region homogenous. Detection of a throat region is then formulated as blob detection on the filled image. Firstly, thresholding is applied on the filled image to reject homogenous region near the spinal cord and mandible. The Hessian matrix is computed for each of the remaining pixels by convolving the image with the second derivatives of a Gaussian kernel with scale  $\sigma$  (here 1), given as Eq (1):

$$H(I(x,y)) = \begin{bmatrix} \frac{\partial^2 I}{\partial x^2} & \frac{\partial^2 I}{\partial x \partial y} \\ \frac{\partial^2 I}{\partial y \partial x} & \frac{\partial^2 I}{\partial y^2} \end{bmatrix} \quad (1)$$

where  $I(x,y)$  is the intensity at pixel  $(x,y)$ . This matrix describes the structure of local intensity variations around each pixel in the image. The eigenvalues also known as characteristic roots of this matrix  $H$  are found using the characteristic equation of  $H$ , given as Eq (2):

$$\det(H - \lambda I) = 0 \quad (2)$$

where  $I$  is 2x2 identity matrix and  $\det(\cdot)$  is the determinant. This Eq (2) is solved to find the eigenvalues  $\lambda$ 's. The corresponding eigenvalues of this matrix are saved as  $\lambda_1$  and  $\lambda_2$ . The critical pixel is analysed based on both eigenvalues of a pixel. Repeated negative eigenvalues indicate that the pixel is a stable sink. Thus, we search for regions of repeated negative eigenvalues and the region with largest repeated eigenvalues is chosen as the throat region. The average pixel of the throat region is calculated and its  $x$  and  $y$  coordinate are saved as  $t_x$  and  $t_y$  respectively.

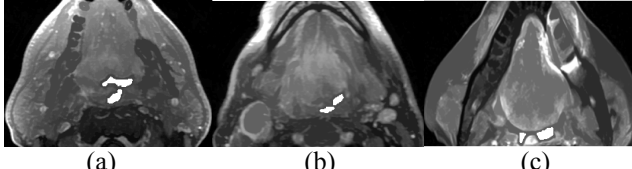


**Fig. 3.** Detected throat region from different MRI slices (white region)

Fig. 3 shows filled images with detected throat regions from different MRI slices. Note that the method is able to detect throat regions of different shapes and also throat region with two parts.

### 2.3. Extraction of tongue base tumour using modified fuzzy c-means (FCM) clustering

The IIH corrected image is input to the modified FCM method described in this section in order to extract the tumour region.

The standard FCM [8] method is an iterative process that produces optimal  $C$  clusters of the grayscale image  $\{I_k\}_{k=1}^N$  where  $N$  is number of pixels, by minimizing the following objective function Eq (3):

$$J_T = \sum_{i=1}^C \sum_{k=1}^N \mu_{ik}^m d^2(v_i, I_k) \quad (3)$$

where  $\{v_i\}_{i=1}^C$  is the prototype intensity of cluster  $C$ . Here  $C$  is the number of tissue types in the image.  $\mu_{ik} \in [0,1]$  is the membership degree of  $k^{th}$  pixel to  $i^{th}$  cluster.  $m (> 1)$  controls the fuzziness of membership function  $\mu_{ik}$ .  $d(v_i, I_k)$  is the Euclidean distance between cluster center  $v_i$  and pixel intensity  $I_k$ . The membership functions are subject to the following constraints Eq (4):

$$\sum_{k=1}^N \mu_{ik} > 0 \quad \forall i \in \{1, \dots, C\}; \quad \sum_{i=1}^C \mu_{ik} = 1 \quad \forall k \in \{1, \dots, N\} \quad (4)$$

This FCM is optimized when high membership values are assigned to pixels close to their centroid and low membership values to the pixels away from the centroid. This standard FCM does not use any information other than distance between the pixel intensity and cluster centres. To improve the capability of this method in order to extract the tumour, information about the spatial location of the tumour is added in its objective function Eq (3). As the tumour is adjacent to the throat region, the squared Euclidean distance from average pixel  $(t_y, t_x)$  of throat region is computed as follows Eq (5):

$$d_s^2(y, x) = \sum_{x=1}^X \sum_{y=1}^Y ((y - t_y)^2 + (x - t_x)^2) \quad (5)$$

where  $x$  and  $y$  are number of columns and number of rows in the image respectively. The purpose of these distance measures is to assign high membership values to the pixels close to the throat region and low values to the pixels away from this region. This distance matrix is converted into one dimensional column-wise vector  $d_s(k)$ .

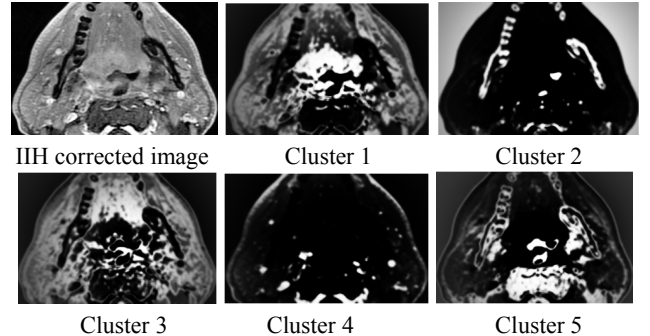


**Fig. 4.** Five clusters of IIH corrected image with visible tongue base tumour in Cluster 1.

This vector is normalized and replicated number of cluster times and saved as  $d_s(i, k)$ . Thus, dimension of  $d_s(i, k)$  is  $C \times N$ .  $d_s(i, k)$  is added to objective function Eq (3) to form a new objective function as follows Eq (6):

$$J_{ST} = \sum_{i=1}^C \sum_{k=1}^N \mu_{ik}^m d^2(v_i, I_k) + \sum_{i=1}^C \sum_{k=1}^N \mu_{ik}^m d_s^2(i, k) \quad (6)$$

Here, membership function  $\mu_{ik}$  is subject to same constraint as in Eq (4). LaGrange multipliers are used to optimize Eq (6) as follows Eq (7):

$$L = \sum_{i=l}^C \sum_{k=l}^N \mu_{ik}^m d^2(v_i, I_k) + \sum_{i=l}^C \sum_{k=l}^N \mu_{ik}^m d_s^2(i, k) + \sum_{k=l}^N \lambda_k (1 - \sum_{i=l}^C \mu_{ik}) \quad (7)$$

The membership functions Eq (8) and cluster centres Eq (9) are updated iteratively as follows:

$$\mu_{ik} = \frac{(d(v_i, I_k) + d_s(i, k))^{-2/(m-1)}}{\sum_{j=1}^C (d(v_j, I_k) + d_s(j, k))^{-2/(m-1)}} \quad (8)$$

$$v_i = \frac{\sum_{k=1}^N \mu_{ik}^m I_k}{\sum_{k=1}^N \mu_{ik}^m} \quad (9)$$

One disadvantage of this modified FCM is that it does not take into account local spatial information of the pixel and is therefore sensitive to noise. In [13] a spatial FCM algorithm which incorporates local spatial information directly into fuzzy membership functions was proposed as Eq (10):

$$\mu'_{ik} = \frac{\mu_{ik}^p h_{ik}^q}{\sum_{j=1}^C \mu_{jk}^p h_{jk}^q} \quad (10)$$

where  $p$  and  $q$  are the control parameters. The spatial function  $h_{ik}$  which compensates membership value of noisy pixel by adding membership values of its neighbouring pixel; is defined as  $h_{ik} = \sum_{l \in Wn} \mu_{il}$  where  $Wn$  is local window ( $5 \times 5$ ) centred at pixel  $k$ . Here, parameter  $p$  was set to 0.1 and  $q$  to 4 for all images. More importance was given

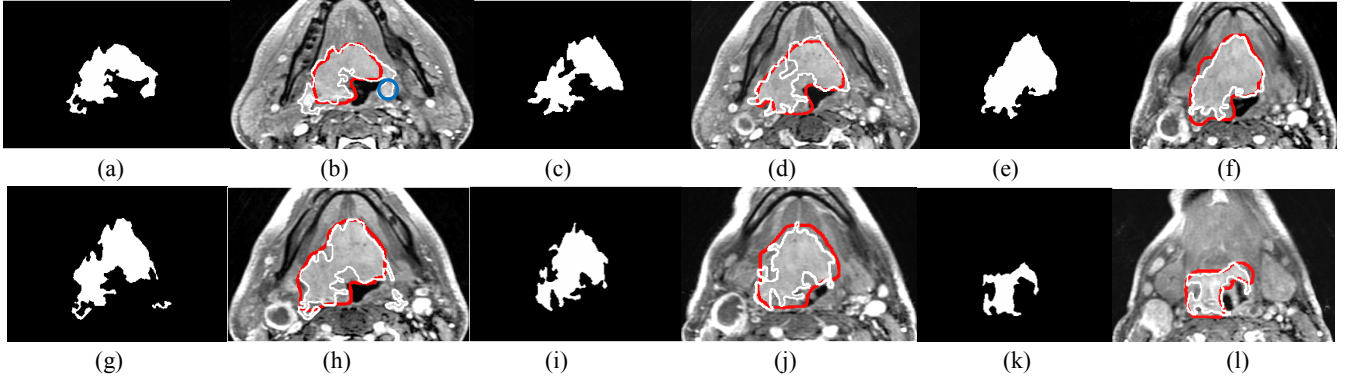


**Fig. 5.** Tumour extraction results: (a) to (l) extracted tumour from automatic algorithm ( $\alpha=0.85$ ) with boundary of tumour: red outline - ground truth (manual boundary drawn by an expert), white outline - obtained by applying Canny edge detector.

**Table 1.** Dice Similarity Coefficient (DSC) for 9 tongue base tumour MRI slices

Slice Number	1	2	3	4	5	6	7	8	9
DSC	0.69	0.81	0.75	0.83	0.82	0.86	0.76	0.74	0.75

to spatial function  $h_{ik}$  to reduce effect of noisy pixels and to get better smoothing effect. Thus, for each iteration after calculating the membership functions using Eq (8) the membership functions are updated using Eq (10) to reduce noisy pixels.

The IIH corrected image is divided into five clusters using this modified FCM method. Fig. 4 shows the IIH corrected image and its five clusters. Cluster 1 in Fig. 4 is the cluster with the tumour region and it can be verified that the tumour region have high membership values. Other clusters in Fig. 4; Cluster 2 to Cluster 5 correspond to other tissue types (like fatty tissues, normal tissues, background) in the IIH corrected image. From these five clusters, the cluster with a tumour region is selected automatically by arranging all five clusters in the descending order of cluster centres (intensities) and selecting the second cluster as the cluster with tumour region. When arranged in descending order first cluster is cluster with fatty tissues (tissues with very high intensity values), second cluster is cluster with tumour region (tissues with high intensity values), third cluster is cluster with normal tissues (medium intensity values), fourth cluster is cluster with tissues of spinal cord (low intensity values) and fifth cluster is cluster with background and air filled region (very low intensity values). The tumour region is separated from second cluster by  $\alpha$ -thresholding the cluster with  $\alpha$ -value of 0.85.

### 3. EXPERIMENTAL RESULTS

MRI scans were performed on patients with visible tongue base tumours before treatment. MRI scans were performed using a GE Medical Systems Signa HDxt 1.5-Tesla scanner. These MR images were obtained with 16-channel, 29-element phased array coils. Other typical imaging parameters were; matrix: 512x512, flip angle: 90°, echo time (TE): 9.2ms, bandwidth: 97.7 Hz/pixel, echo train length: 3, slice thickness: 3.5mm, spacing between slices:

4.5mm. The algorithm was evaluated on these real MRI data sets.

The algorithm was implemented in Matlab 2013a on a Windows machine with Intel Pentium Dual-Core 2.5 GHz processor. 9 sequential short axis (SA) T1+Gd MR images with visible tongue base tumour were selected to validate the robustness of the algorithm. The throat region was detected successfully on all 9 MR images. For the evaluation of the tumour region, comparison was made between automatic and manual extraction results. Tumours were extracted automatically for 9 selected MRI slices using the proposed algorithm and manually from a consultant clinical oncologist with expertise in upper gastrointestinal (GI) radiotherapy. Fig. 5(a) to 5(l) shows automatic tumour extraction from 6 MRI slices. The boundary of the tumour region is obtained by applying a Canny edge detector on the automatic extracted tumour region and superimposed with manual extraction results (5(a) to 5(l)). The dice similarity coefficient (DSC) [14] is calculated for a tumour region of 9 slices. High values of DSC indicate good agreement between automatic and manual extraction results. For 9 slices average DSC is  $0.77 \pm 0.08$ . Table 1 shows the DSC for all 9 slices. The average area difference in percentage (%) for 9 slices is 17.08 with the manually extracted tumour area used as reference. This difference in the results between manual and automatic extraction can be explained as in some slices where tumours split into two parts manual extraction picks only bulky part and leaves out the small part (Fig. 5(b) (shown in circle)) whereas the automatic

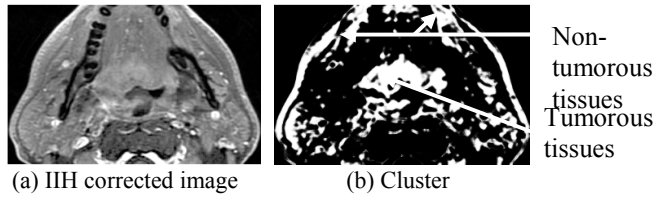


**Fig. 6.** (a) IIH corrected image and (b) Cluster with tumour region obtained using standard FCM.

algorithm picks both parts. In some slices where the tumour boundary is unclear, the manual extraction picks the boundary of the tumour with a certain margin (Fig. 5(j)) whereas the automatic algorithm extract tumour region without any margin.

A comparison of this modified FCM technique was made with standard FCM [8] technique. Fig. 6 shows IIH corrected image and the Cluster image with tumour region obtained using standard FCM. This can be compared to Cluster 1 from Fig.4. In standard FCM technique tissues away from throat region are assigned high membership values similar to the tumorous tissues near throat region as they have similar intensity values as tumorous tissues. Thus, it is difficult to separate tumour region from cluster using simple technique like  $\alpha$ -thresholding. However, in modified FCM technique, due to additional distance measures, non-tumorous tissues away from throat region are assigned low membership values. Thus, tumour region can be separated from cluster using  $\alpha$ -thresholding.

#### 4. CONCLUSIONS AND FUTURE WORK

This paper presented a new automatic tongue base tumour extraction algorithm for T1+Gd MR images. In this algorithm the throat region, known to be close to the common site of tumour region, was detected using Hessian analysis. A new objective function for a FCM was devised by adding a distance measure created from average pixel of throat region to extract tumour region. Local spatial information of pixel is considered in this modified FCM to reduce its sensitivity to noise. The proposed algorithm successfully extracts the tumour region with different shapes, size, unclear boundaries without any manual interaction. The comparison with manual extraction results shows that, the algorithm with further enhancement can be used to assist in radiotherapy and surgery planning.

Future work will focus on refining current methods using techniques such as deformable models. The current algorithm focusses on the extraction of tumours from 2-dimensional MR image. Future work will concentrate on 3-dimensional segmentation and visualisation of tongue base tumour.

#### 5. ACKNOWLEDGEMENT

The authors would like to acknowledge the Beatson Oncology Fund for their financial support with this study.

#### 6. REFERENCES

- [1] A. Kreimer et al., "Evaluation of human papillomavirus antibodies and risk of subsequent head and neck cancer", *J. Clin. Oncol.*, vol. 31, no. 21, pp. 2708-2715, July 2013
- [2] J. Watkinson and R. Gilbert, *Stell and Maran's Textbook of Head and Neck Surgery and Oncology*, Fifth Edition, London, UK: Hodder Arnold, chapter 31, pp. 616, 2012
- [3] T. Doshi, J. Soraghan, L. Petropoulakis, D. Grose and K. MacKenzie "Semi-Automatic Segmentation of Tongue Tumors from Magnetic Resonance Imaging", in *Proc. of 20th IEEE IWSSIP conference*, Bucharest, Romania, pp. 143-146, July 2013
- [4] L. Fletcher, L. Hall, D. Goldgof and F. Reed, "Automatic segmentation of non-enhancing brain tumors in magnetic resonance images", *Artif Intell Med*, vol. 21, issue 1-3, pp. 43-63, 2001
- [5] A. Hamamci, N. Kucuk, K. Karaman, K. Engin, and G. Unal, "Tumor-Cut: Segmentation of Brain Tumors on Contrast Enhanced MR Images for Radiosurgery Applications", *IEEE Trans. on Medical Imaging*, vol. 31, no. 3, pp. 790-804, March 2012
- [6] I. Despotovic, E. Vansteenkiste, and W. Philips, "Spatially Coherent Fuzzy Clustering for Accurate and Noise-Robust Image Segmentation", *IEEE Signal Processing Letters*, vol. 20, no. 4, pp. 295-298, April 2013
- [7] C. Hung, S. Kulkarni, and B. Kuo, "A New Weighted Fuzzy C-Means Clustering Algorithm for Remotely Sensed Image Classification", *IEEE Journal of Selected Topics in Signal Processing*, vol. 5, no. 3, pp. 543-553, June 2011
- [8] J. Bezdek, *Pattern Recognition with Fuzzy Objective Function Algorithms*. New York: Plenum, 1981.
- [9] M. Ahmed, S. Yamany, N. Mohamed, A. Farag, and T. Moriarty, "A Modified Fuzzy C-Means Algorithm for Bias Field Estimation and Segmentation of MRI Data", *IEEE Trans. on Medical Imaging*, vol. 21, no. 3, pp. 539-552, March 2002
- [10] A. Simmons, P. Tofts, G. Barker and S. Arridge, "Sources of Intensity Nonuniformity in Spin Echo Images at 1.5 T", *Magn. Reson. Med.*, vol. 32, no. 1, pp. 121-128, 1994
- [11] O. Salvado, C. Hillenbrand, S. Zhang, and D. Wilson, "Method to Correct Intensity Inhomogeneity in MR Images for Atherosclerosis Characterization", *IEEE Trans. on Medical Imaging*, vol. 25, no. 5, pp. 539-552, May 2006
- [12] P. Soille, *Morphological Image Analysis: Principles and Applications*, Springer-Verlag, pp. 173-174, 1999
- [13] K. Chuang, H. Hzeng, S. Chen, J. Wu and T. Chen "Fuzzy c-means clustering with spatial information for image segmentation", *Computerized Medical Imaging and Graphics*, vol. 30, pp. 9-15, 2006
- [14] L. Dice, "Measures of the amount of ecological association between species" *Ecology*, vol. 26, no. 3, pp. 297-302, July 1945